

STDP-based Associative Memory Formation and Retrieval

Hong-Gyu Yoon* and Pilwon Kim†

Department of Mathematical Sciences
Ulsan National Institute of Science and Technology(UNIST)
Ulsan Metropolitan City
44919, Republic of Korea

August 10, 2021

Abstract

Spike-timing-dependent plasticity(STDP) is a biological process in which the precise order and timing of neuronal spikes affect the degree of synaptic modification. While there has been numerous research focusing on the role of STDP in neural coding, the functional implications of STDP at the macroscopic level in the brain have not been fully explored yet. In this work, we propose a neurodynamical model based on STDP that renders storage and retrieval of a group of associative memories. We showed that the function of STDP at the macroscopic level is to form a “memory plane” in the neural state space which dynamically encodes high dimensional data. We derived the analytic relation between the input, the memory plane, and the induced macroscopic neural oscillations around the memory plane. Such plane produces a limit cycle in reaction to a similar memory cue, which can be used for retrieval of the original input.

Introduction

Spike-timing-dependent plasticity(STDP), as a synaptic modification rule according to the order of pre- and post-synaptic spiking within a critical time window, has been demonstrated in the nervous systems over a wide range of species from insects to humans. STDP is considered to be critical for understanding the cognitive mechanisms such as learning of temporal sequences [1, 2], formation of associative memory [3, 4] and manipulation of existing memory [5–7]. Despite such progress and findings, the question still remains open as to how STDP affects the distributed process of information at the macroscopic level in the brain.

Modeling macroscopic brain activity with nonlinear dynamical systems facilitates understanding of brain functions [8–10]. The hypothesis of storing memory in a form of an attractor of the dynamics is now accepted with substantial supporting evidence [11–16]. However, it is still unclear how specific trajectories of neural states could emerge through neural plasticity.

*hkyoon@unist.ac.kr

†pwkim@unist.ac.kr, *corresponding author*

In this work, we propose that a neurodynamical function of STDP is related to storage and retrieval of associative memories at a macroscopic scale. When the system is excited by a repeating sequence, STDP create a circular set of directed connections inducing neural oscillations in the neural state space. While the neural state space is extremely high dimensional, the oscillations are confined in a two-dimensional plane which we call *memory plane*. Such memory plane can act as a generator of a limit cycle in reaction to an external input. That is, once the system converges under a sequential memory input and forms the corresponding memory plane, it produces a limit cycle in reaction to a similar memory cue, which can be used for retrieval of the original input.

The presence and the function of such planar memory structure in the neural state space have caught attention in [17], where it has been proposed that STDP can store transient inputs as imaginary-coded memories. In this work, we formalized the concept of the memory plane and the retrievability of neural states to analyze how data is effectively stored in the neural state space. We derived the analytic relation between the input, the memory plane, and the induced macroscopic neural oscillations around the memory plane. This enables us to understand the functional role of STDP in terms of neurodynamical systems and view the macroscopic neural oscillations in the brain as circulations across the memory representations. The analytic results in this paper suggest an alternative method to store and retrieve high-dimensional and strongly associated data sets in analog devices. In the separate work [18], we proposed a practical encoding algorithm based on the analysis done in this article to store associate image/text data sets into retrievable neural states.

Model Setups

Firing-Rate Neural Network with STDP

Our work follows the framework of standard firing-rate models [17, 19]. We set the differential equation for the neural state as

$$\dot{\mathbf{x}} = -\mathbf{x} + \mathbf{W}\phi(\mathbf{x}) + \mathbf{b}(t), \quad (1)$$

where $\mathbf{x} = [x_1 \cdots x_N]^\top \in \mathbb{R}^N$ is the state of N neuronal nodes and $\mathbf{W} = (W_{ij}) \in \mathbb{R}^{N \times N}$ is a connectivity matrix with W_{ij} corresponding to the strength of synaptic connection from node j to i . Here ϕ is a regularizing transfer function and $\mathbf{b}(t)$ is a sensory memory input.

The mechanism of STDP can be formulated as [20]

$$\begin{aligned} \dot{W}_{ij}(t) = -\gamma W_{ij}(t) + \rho \left(\underbrace{\int_0^\infty K(s)\phi(x_j(t-s))\phi(x_i(t)) ds}_{\text{pre- to post- firing}} \right. \\ \left. + \underbrace{\int_0^\infty K(-s)\phi(x_j(t))\phi(x_i(t-s)) ds}_{\text{post- to pre- firing}} \right), \quad (2) \end{aligned}$$

where K is a temporal kernel. The parameters γ and ρ are the decaying rate of homeostatic plasticity and the learning rate, respectively.

For analytic simplicity, we use $\phi(\mathbf{x}) = \mathbf{x}$ and a Dirac-delta kernel $K(s)$ defined as

$$K(s) := \begin{cases} \delta(s - s_0) & s > 0 \\ -\delta(s + s_0) & s \leq 0, \end{cases} \quad (3)$$

with $s_0 > 0$. After simplifications, the main model becomes

$$\boxed{\begin{cases} \dot{\mathbf{x}} = -\mathbf{x} + \mathbf{W}\mathbf{x} + \mathbf{b}(t) \\ \dot{\mathbf{W}} = -\gamma\mathbf{W} + \rho(\mathbf{x}\mathbf{x}_\tau^\top - \mathbf{x}_\tau\mathbf{x}^\top) \end{cases}} \quad (4)$$

where $\mathbf{x}_\tau = \mathbf{x}(t - \tau)$ stands for delayed synaptic response. More detailed derivation of the evolution rule for \mathbf{W} can be found in Appendix A.

Storage and Retrieval Phases

Let $\mathbf{m}_1, \dots, \mathbf{m}_n \in \mathbb{R}^N$, and each \mathbf{m}_i be memory representations which are encoded from some external sensory inputs and are to be stored in the system (4). We assume in the storage phase that the input $\mathbf{b}(t)$ takes a form of sequential oscillatory drive

$$\boxed{\mathbf{b}(t) = \sum_{i=1}^n \sin(\omega t - \xi_i) \mathbf{m}_i, \quad 0 \leq \xi_1 < \dots < \xi_n < \pi,} \quad (5)$$

where ω stands for the frequency of neural oscillations and $\xi_i, i = 1, \dots, n$ stands for the sampling time for each representation. In the next section, we will show that the synaptic connectivity $\mathbf{W}(t)$ converges to a certain constant matrix \mathbf{W}^* that reflects the informations of memory representations $\mathbf{m}_1, \dots, \mathbf{m}_n$.

In the *retrieval phase*, change in synaptic weights is suppressed (i.e., $\gamma = \rho = 0$) as

$$\boxed{\dot{\mathbf{x}} = -\mathbf{x} + \mathbf{W}^*\mathbf{x} + \mathbf{b}_c(t),} \quad (6)$$

where $\mathbf{b}_c(t)$ is the cue input in the form of

$$\boxed{\mathbf{b}_c(t) = \sin \omega t \mathbf{m}_c, \quad \mathbf{m}_c \in \mathbb{R}^N.} \quad (7)$$

We are interested in how the original representations can be revived from the neural activity $\mathbf{x}(t)$ when $\mathbf{m}_c \in \mathbb{R}^N$ is close to one of the memory representations. Figure 1a and b illustrate the setup for storage and retrieval process through the systems (4) and (6), respectively.

Robust Learning by STDP

This section presents some analytical results on the storage phase. We first confirm that the sensory input in Eq. (5) resides in a plane in \mathbb{R}^N , a *memory plane*, which is defined in the following lemma.

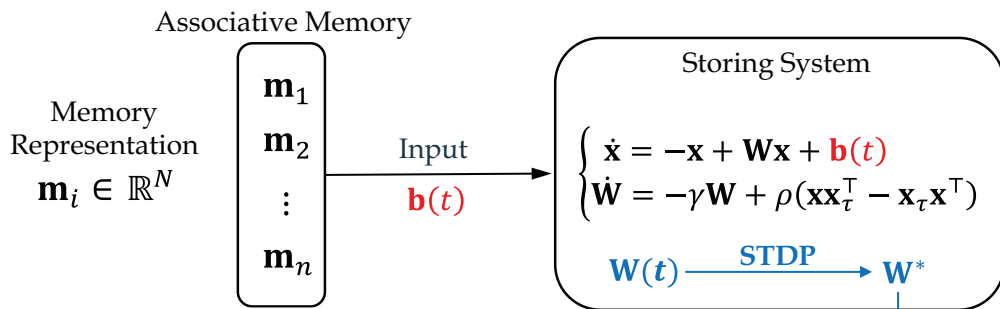
Lemma A. $\mathbf{b}(t)$ is periodic and embedded in a plane $S := \text{Span}\{\mathbf{u}, \mathbf{v}\}$ where

$$\mathbf{u} = -\Psi \sin \boldsymbol{\xi} \quad \text{and} \quad \mathbf{v} = \Psi \cos \boldsymbol{\xi}. \quad (8)$$

Here $\Psi = [\mathbf{m}_1 | \dots | \mathbf{m}_n] \in \mathbb{R}^{N \times n}$, $\sin \boldsymbol{\xi} = [\sin \xi_1 \ \dots \ \sin \xi_n]^\top \in \mathbb{R}^n$, and $\cos \boldsymbol{\xi} = [\cos \xi_1 \ \dots \ \cos \xi_n]^\top \in \mathbb{R}^n$.

The following theorem asserts the existence of the periodic solutions $(\mathbf{x}^*(t), \mathbf{W}^*)$ of the system (4) in terms of the memory plane S .

a Storage Phase



b Retrieval Phase

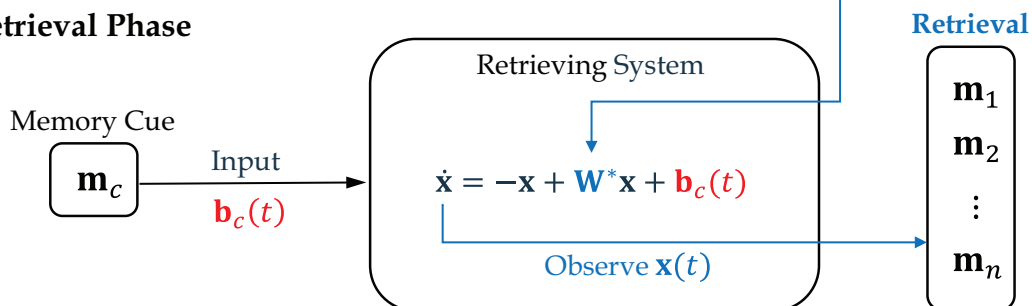


Figure 1: Description of the associative memory process for storage and retrieval of sensory input informations. **(a)** Storage phase: The STDP-based system processes the memory representations $\{\mathbf{m}_i\}_{i=1}^n$ and the connectivity matrix $\mathbf{W}(t)$ converges to a constant connectivity \mathbf{W}^* as a result. **(b)** Retrieval phase: A memory cue input $\mathbf{b}_c(t)$ triggers the retrieval of the original inputs through the connectivity \mathbf{W}^* acquired in the storage phase.

Theorem 1. (PERIODIC SOLUTION WITH STEADY CONNECTIVITY) *The system (4) under input (5) has a periodic solution $\mathbf{x}^*(t)$ with a constant connectivity matrix \mathbf{W}^* , where*

$$\mathbf{x}^*(t) \in S \text{ for all } t, \quad \text{and} \quad \mathbf{W}^* \in \wedge^2(S). \quad (9)$$

Here, $\wedge^2(S)$ indicates an exterior power of S , which is a set of anti-symmetric matrices in the form of $\alpha(\mathbf{v}\mathbf{u}^\top - \mathbf{u}\mathbf{v}^\top)$ for any vectors \mathbf{u} and \mathbf{v} in S . The exact analytic form of such $(\mathbf{x}^*(t), \mathbf{W}^*)$ can be found in Appendix B2. Figure 2 illustrates the convergence of the neural activity toward a periodic orbit $\mathbf{x}^*(t)$ on memory plane S as described in Theorem 1. Note that the memory plane S does not necessarily contain the memory representations $\mathbf{m}_1, \dots, \mathbf{m}_n$ in general. However, we show in the next section that S is likely located close to the memory representations in the high dimensional neural state space.

To investigate the stability of $(\mathbf{x}^*(t), \mathbf{W}^*)$ found in Theorem 1, we perform the analysis on the maximal Lyapunov exponent (MLE) [21, 22]. Setting $\mathbf{x}(t) = \mathbf{x}^*(t) + \delta\mathbf{x}(t)$ and $\mathbf{W}(t) = \mathbf{W}^* + \delta\mathbf{W}(t)$, we acquire a variational equation from Eq. (4) as

$$\begin{cases} \delta\dot{\mathbf{x}} = (-\mathbf{I} + \mathbf{W}^*)\delta\mathbf{x} + \delta\mathbf{W}\mathbf{x}^* \\ \delta\dot{\mathbf{W}} = -\gamma\delta\mathbf{W} + \rho(\delta\mathbf{x}\mathbf{x}_t^{*\top} - \mathbf{x}_t^*\delta\mathbf{x}^\top + \mathbf{x}^*\delta\mathbf{x}_t^\top - \delta\mathbf{x}_t\mathbf{x}^{*\top}). \end{cases} \quad (10)$$

The derivation of Eq. (10) and the detailed computational method for estimating MLE can be found in Appendix C1 and C2, respectively. Fig. 3 shows the color plot of numerically estimated MLE of Eq. (4). For the regions showing negative values of MLE, one can assure

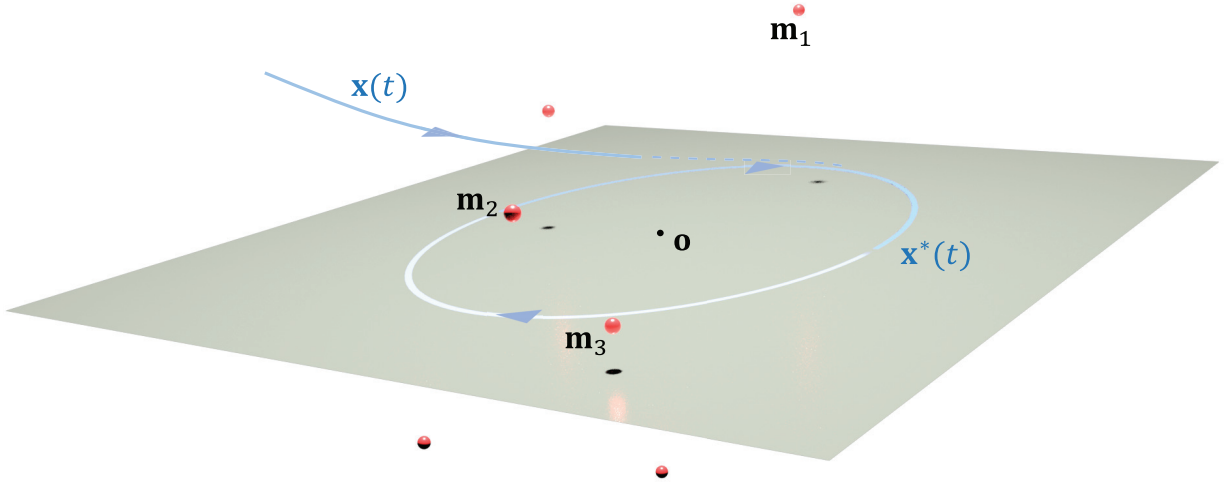


Figure 2: Illustrative image describing the convergence toward the periodic solution in Theorem 1. Each red circle represents the position of each memory representation \mathbf{m}_i in the neural state space \mathbb{R}^N . The memory plane S is located close to the memory representations and plays a role of an attractor that brings $\mathbf{x}(t)$ to a periodic orbit $\mathbf{x}^*(t)$.

that the solution $(\mathbf{x}^*(t), \mathbf{W}^*)$ is an attractor, thus consequently achieving a robust learning for any types of input of form Eq. (5).

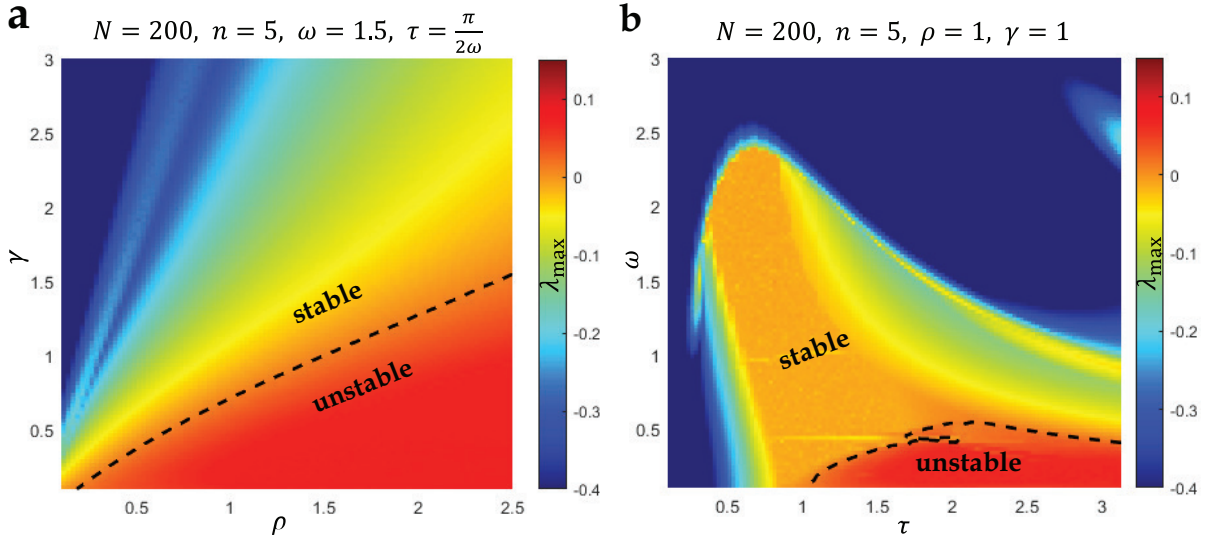


Figure 3: Plot of numerically estimated maximal Lyapunov exponent (λ_{\max}) of Eq (4), under input (5) in the storage phase. **(a)** Color plot of λ_{\max} for parameter $(\rho, \gamma) \in [0.1, 2.5] \times [0.1, 3]$ for system with number of nodes $N = 200$ under input of 5 unit length normalized memory representations and $\omega = 1.5$, $\tau = \frac{\pi}{2\omega}$. The unstable region tends to be confined in $\gamma \leq \alpha\rho$ with some $\alpha \approx 0.7$. **(b)** Plot of λ_{\max} for parameter $(\tau, \omega) \in [0.1, \pi] \times [0.1, 3]$ for system with number of nodes $N = 200$ under input of 5 unit length normalized memory representations and $\gamma = \rho = 1$. For both plot, generally, the stable/unstable regions are hardly affected by the size of the system N . On the other hand, unstable regions tends to grow larger if the size of the input $\mathbf{b}(t)$ (or analogously, the number of memory representations n) increases.

Auto-associative Retrieval by a Memory Cue

In this section, we provide the analysis on Eq. (6) under cue input Eq. (7). We propose that the convergent synaptic connectivity \mathbf{W}^* acquired from the storage phase effectively contains the information of a whole set of memory representations $\{\mathbf{m}_i\}_{i=1}^n$ and leads to periodic retrieval of them.

Let us define a **retrievable subspace** $\mathcal{M} := \text{Span}\{\mathbf{m}_i\}_{i=1}^n$ with respect to a set of memory representations $\{\mathbf{m}_i\}_{i=1}^n$. A neural state $\mathbf{x} \in \mathbb{R}^N$ is said to be **retrievable** with respect to $\{\mathbf{m}_i\}_{i=1}^n$, if $\mathbf{x}(t) \in \mathcal{M} \setminus \{\mathbf{0}\}$. Note that the memory plane S is a subset of the retrievable subspace \mathcal{M} (see Eq. (8)). In the separate work [18], we work on a practical implementation of the system (4) with some encoding/decoding processes, and show that a series of external sensory data can be recovered from a retrievable state $\mathbf{x}(t)$ as long as they are properly encoded into the memory representations $\{\mathbf{m}_i\}_{i=1}^n$. Refer to Discussion section for more about decoding of retrievable states.

The following theorem states that for some appropriately chosen memory cue representation \mathbf{m}_c , there is a specific moment $t = t^\dagger$ at which the corresponding neural state $\mathbf{x}(t)$ becomes retrievable.

Theorem 2. (PERIODIC RETRIEVAL) *For any non-zero cue \mathbf{m}_c , the solution of Eq. (6) under input (7) asymptotically approaches to some periodic solution $\mathbf{x}_r^*(t)$. Especially if $\mathbf{m}_c \notin S_\perp$, $\mathbf{x}_r^*(t)$ becomes periodically retrievable at $t = t^\dagger > 0$ where*

$$t^\dagger = \frac{1}{\omega} \tan^{-1} \omega + n \frac{\pi}{\omega}, \quad n \in \mathbb{Z}. \quad (11)$$

Note that, since the retrieval dynamics $\mathbf{x}_r(t)$ is attracted to a limit cycle $\mathbf{x}_r^*(t)$, its retrievability depends on that of $\mathbf{x}_r^*(t)$. The minimal condition for the retrievability mentioned in Theorem 2 can be extended further: the proximity of \mathbf{m}_c to S and \mathcal{M} determines the retrievability of $\mathbf{x}_r^*(t)$ as follows.

- (i) Case $\mathbf{m}_c \in \mathcal{M}$ (good cue): $\mathbf{x}_r^*(t) \in \mathcal{M}$ for all t .
- (ii) Case $\mathbf{m}_c \in S_\perp \cap \mathcal{M}^c$ (relavent cue): $\mathbf{x}_r^*(t)$ is retrievable at $t = t^\dagger$ as in Theorem 2.
- (iii) Case $\mathbf{m}_c \in S_\perp \cap \mathcal{M}^c$ (wrong cue): $\mathbf{x}_r^*(t)$ never becomes retrievable.

Fig. 4 gives a graphical illustration about dependence of the retrieval dynamics on the memory cue. More details about the retrievability conditions including the proof of Theorem 2 can be found in Appendix B3.

From the above analysis, one can see that the chance for good and relavent cues increases if the memory plane S is formed near the memory representations $\mathbf{m}_1, \dots, \mathbf{m}_n$. To measure the distance between S and each memory representation \mathbf{m}_i , one can use the mean cosine similarity $\langle \cos \theta_i \rangle_i$ where θ_i represents the angle between each \mathbf{m}_i and S . Note that if $\langle \cos \theta_i \rangle_i = 1$ if all $\mathbf{m}_1, \dots, \mathbf{m}_n$ are embedded in S . The next theorem tells that one can choose the optimal sampling time for input ξ_1, \dots, ξ_n in Eq. (5).

Theorem 3. (OPTIMAL CHOICE FOR ξ_i) *Suppose $\{\mathbf{m}_i\}_{i=1}^n$ with $\mathbf{m}_i \in \mathbb{R}^N$ are mutually orthogonal vectors of the same magnitude. Then the maximum value of $\langle \cos \theta_i \rangle_i$ is $\sqrt{\frac{2}{n}}$ and can be attained with the the distribution of ξ_i as*

$$\xi_i = (i-1) \frac{\pi}{n} + \alpha, \quad i = 1, \dots, n, \quad 0 \leq \alpha < \frac{\pi}{n}. \quad (12)$$

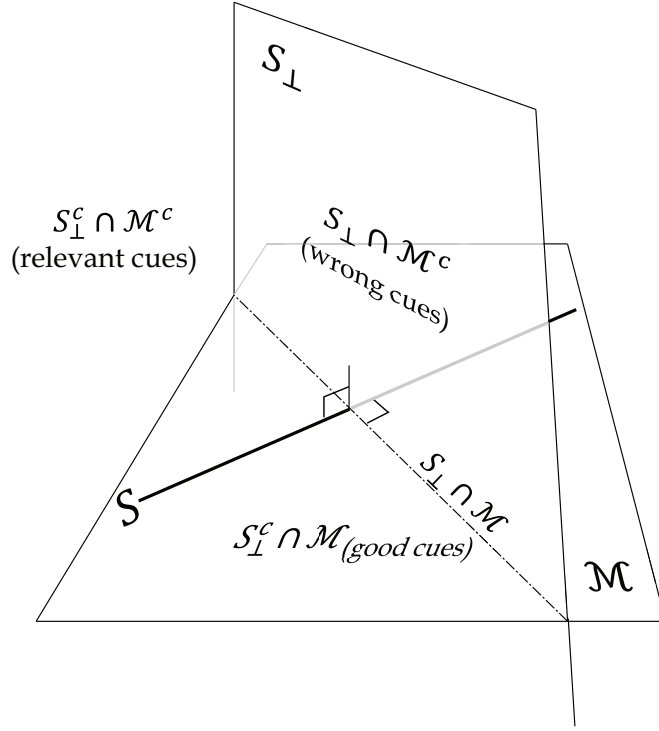


Figure 4: For the intuitive graphical understanding, the retrieval subspace \mathcal{M} and the memory plane S are visualized as a plane and an embedded line, respectively. (i) Case $\mathbf{m}_c \in \mathcal{M}$ (good cue): $\mathbf{x}_r^*(t) \in \mathcal{M}$ for all t . (ii) Case $\mathbf{m}_c \in S_{\perp} \cap \mathcal{M}^c$ (relevant cue): $\mathbf{x}_r^*(t)$ is retrievable at $t = t^{\dagger}$ as in Theorem 2. (iii) Case $\mathbf{m}_c \in S_{\perp} \cap \mathcal{M}^c$ (wrong cue): $\mathbf{x}_r^*(t)$ never becomes retrievable.

The theorem suggests a uniform sampling times ξ_i for the sequential input of representations in order to naturally maximize the expected performance of retrieval.

Discussion

There are now substantial evidences accumulated that such macroscopic neural oscillations are related to memory encoding, attention, and integration of visual patterns [23–25]. Our analysis supports such functional role of neural oscillations, by viewing them as limit cycles related to a memory plane which stores the information in the form of an anti-symmetric connectivity. We were able to show that the performance of retrieval is determined by the similarity of a memory cue to the original data. This suggests an alternative computational approach that can handle high dimensional and strongly associated data sets from a biomimetic perspective.

The cognitive systems do not simply receive an external input in a passive way, but rather actively pose it on acceptance. It is therefore reasonable to assume that there is some pre-encoding process to encode the external inputs, say, $\mathbf{f}_1, \dots, \mathbf{f}_n$ into the memory components $\mathbf{m}_1, \dots, \mathbf{m}_n$ in the neural state space. To model such preprocess, one can use a set of internal tag vectors $\mathbf{r}_1, \dots, \mathbf{r}_n$. For example, one of possible ways of encoding is to use tensor product like $\mathbf{m}_i = \mathbf{f}_i \otimes \mathbf{r}_i$. Then the tag vectors can be also used for decoding $\mathbf{x}(t)$, that is, to retrieve the external inputs $\mathbf{f}_1, \dots, \mathbf{f}_n$ from $\mathbf{x}(t)$, while $\mathbf{x}(t)$ is retrievable. In the separate paper, we will study the end-to-end memory process with encoding/decoding processes, focusing on more practical issues such as how the network can embed actual data into neural representations for efficient reproduction from the retrievable states.

Acknowledgements

P. Kim was supported by National Research Foundation of Korea (2017R1D1A1B04032921) and H. Yoon was supported by Ulsan National Institute of Science and Technology 12(1.200052.01).

Appendix A: Derivation of the STDP Learning Rule

Actually, Eq. (2) in the main text can be equivalently written by the following expression only using convolution defined on \mathbb{R} , i.e.,

$$\dot{W}_{ij}(t) = -\gamma W_{ij}(t) + \rho((K_{\Delta t > 0} * \phi(x_j))(t)\phi(x_i)(t) + (K_{\Delta t \leq 0} * \phi(x_i))(t)\phi(x_j)(t)), \quad (13)$$

where $K_{\Delta t > 0}(s)$ comes from the kernel $K(s)$ with $s > 0$ only, and $K_{\Delta t \leq 0}(s)$ is $K(-s)$ with $s \leq 0$ only. Therefore, in the case of kernels only behaving as Eq. (3), we have $K_{\Delta t > 0}(s) = \delta(s - s_0) = \delta_{s_0}(s)$ and $K_{\Delta t \leq 0}(s) = -\delta(-s + s_0) = -\delta(s - s_0) = -\delta_{s_0}(s)$. Now, since $(\delta_{s_0} * f)(t) = \int_{\mathbb{R}} \delta(s - s_0) f(t - s) ds = f(t - s_0)$, thus the terms in Eq. (13) including convolution is simplified into

$$\dot{W}_{ij}(t) = -\gamma W_{ij}(t) + \rho(\phi(x_j(t - s_0))\phi(x_i(t)) - \phi(x_i(t - s_0))\phi(x_j(t))). \quad (14)$$

Rewriting it in matrix form,

$$\dot{\mathbf{W}}(t) = -\gamma \mathbf{W}(t) + \rho(\phi(\mathbf{x}(t))\phi(\mathbf{x}(t - s_0))^\top - \phi(\mathbf{x}(t - s_0))\phi(\mathbf{x}(t))^\top). \quad (15)$$

Now, if one specifies s_0 with some $s_0 = \tau > 0$ and applies approximation $\phi(x) \approx x$, then Eq. (15) concisely reduces to

$$\dot{\mathbf{W}} = -\gamma \mathbf{W} + \rho(\mathbf{x}\mathbf{x}_\tau^\top - \mathbf{x}_\tau\mathbf{x}^\top) \quad (16)$$

with introducing notation $\mathbf{x}_\tau = \mathbf{x}(t - \tau)$ as in the main text. This is our evolution equation on $\dot{\mathbf{W}}$, where the term $-\gamma \mathbf{W}$ acts as homeostatic decay and $\rho(\mathbf{x}\mathbf{x}_\tau^\top - \mathbf{x}_\tau\mathbf{x}^\top)$ acts as actual learning operator by STDP. \blacksquare

Appendix B: Proofs for the Theoretical Results

B1: Proof of Lemma A

Let $\mathbf{b}(t) = [b_1(t) \ \cdots \ b_N(t)]^\top$, and $\mathbf{m}_i = [m_{i_1} \ \cdots \ m_{i_N}]^\top$. Then, each component of $\mathbf{b}(t)$ satisfies

$$\begin{aligned} b_j(t) &= \sum_{i=1}^n m_{i_j} \sin(\omega t - \xi_i) \\ &= \sum_{i=1}^n m_{i_j} (\sin \omega t \cos \xi_i - \cos \omega t \sin \xi_i) \\ &= \cos \omega t \left(\sum_i m_{i_j} (-\sin \xi_i) \right) + \sin \omega t \left(\sum_i m_{i_j} \cos \xi_i \right), \quad j = 1, \dots, N. \end{aligned} \quad (17)$$

Thus if we introduce

$$\begin{cases} \mathbf{u} = - \left[\sum_{i=1}^n m_{i_1} \sin \xi_i & \cdots & \sum_{i=1}^n m_{i_N} \sin \xi_i \right]^\top \\ \mathbf{v} = \left[\sum_{i=1}^n m_{i_1} \cos \xi_i & \cdots & \sum_{i=1}^n m_{i_N} \cos \xi_i \right]^\top, \end{cases} \quad (18)$$

then this choice of \mathbf{u}, \mathbf{v} can be represented in alternate form of $\mathbf{u} = -\Psi \sin \xi$ and $\mathbf{v} = \Psi \cos \xi$ where Ψ , $\sin \xi$, and $\cos \xi$ are defined as in the theorem statement, and guarantees

$$\mathbf{b}(t) = \cos \omega t \mathbf{u} + \sin \omega t \mathbf{v} \quad (19)$$

by Eq. (17). Therefore $\mathbf{b}(t)$ is periodic and embedded in plane $\text{Span}\{\mathbf{u}, \mathbf{v}\}$. \blacksquare

B2: Proof of Theorem 1

The proof of this theorem requires the following lemma which describes some algebraic relations of frequently appearing periodic functions in the behavior of neural periodic solution $\mathbf{x}^*(t)$.

Lemma B. Let $c_{i,[\lambda,\omega]}(t)$ be the following periodic functions in t , with parameters $\lambda, \omega \in \mathbb{R}^+$, which is defined as

$$\begin{cases} c_{1,[\lambda,\omega]}(t) = \frac{1}{2} \left(\frac{\cos(\omega t - \theta_{-,[\lambda,\omega]})}{\sqrt{\Phi_{-,[\lambda,\omega]}}} + \frac{\cos(\omega t - \theta_{+,[\lambda,\omega]})}{\sqrt{\Phi_{+,[\lambda,\omega]}}} \right) \\ c_{2,[\lambda,\omega]}(t) = \frac{1}{2} \left(\frac{\sin(\omega t - \theta_{-,[\lambda,\omega]})}{\sqrt{\Phi_{-,[\lambda,\omega]}}} - \frac{\sin(\omega t - \theta_{+,[\lambda,\omega]})}{\sqrt{\Phi_{+,[\lambda,\omega]}}} \right) \\ c_{3,[\lambda,\omega]}(t) = \frac{1}{2} \left(\frac{\sin(\omega t - \theta_{-,[\lambda,\omega]})}{\sqrt{\Phi_{-,[\lambda,\omega]}}} + \frac{\sin(\omega t - \theta_{+,[\lambda,\omega]})}{\sqrt{\Phi_{+,[\lambda,\omega]}}} \right) \\ c_{4,[\lambda,\omega]}(t) = -\frac{1}{2} \left(\frac{\cos(\omega t - \theta_{-,[\lambda,\omega]})}{\sqrt{\Phi_{-,[\lambda,\omega]}}} + \frac{\cos(\omega t - \theta_{+,[\lambda,\omega]})}{\sqrt{\Phi_{+,[\lambda,\omega]}}} \right), \end{cases} \quad (20)$$

where $\theta_{\pm,[\lambda,\omega]} = \tan^{-1}(\omega \pm \lambda)$, $\Phi_{\pm,[\lambda,\omega]} = \lambda^2 \pm 2\omega\lambda + \omega^2 + 1$. Let's denote $\frac{d}{dt}c_{i,[\lambda,\omega]}(t)$ with $\dot{c}_{i,[\lambda,\omega]}(t)$. Then, the followings are true:

1. $\dot{c}_{1,[\lambda,\omega]} = -\omega c_{3,[\lambda,\omega]}$, $\dot{c}_{2,[\lambda,\omega]} = -\omega c_{4,[\lambda,\omega]}$, $\dot{c}_{3,[\lambda,\omega]} = \omega c_{1,[\lambda,\omega]}$, and $\dot{c}_{4,[\lambda,\omega]} = \omega c_{2,[\lambda,\omega]}$.
2. **a.** $c_{1,[\lambda,\omega]}(t) - \omega c_{3,[\lambda,\omega]}(t) + \lambda c_{2,[\lambda,\omega]}(t) = \cos \omega t$.
b. $c_{1,[\lambda,\omega]}(t) + \omega c_{3,[\lambda,\omega]}(t) + \lambda c_{4,[\lambda,\omega]}(t) = \sin \omega t$.
c. $c_{2,[\lambda,\omega]}(t) - \omega c_{4,[\lambda,\omega]}(t) - \lambda c_{1,[\lambda,\omega]}(t) = 0$.
d. $c_{2,[\lambda,\omega]}(t) + \omega c_{4,[\lambda,\omega]}(t) - \lambda c_{3,[\lambda,\omega]}(t) = 0$.

Proof. Statement 1 can be straightforwardly shown by direct differentiation. For statement 2, omitting the $[\lambda,\omega]$ notations in $\theta_{\pm,[\lambda,\omega]}$, observe that

$$\begin{aligned} & c_{1,[\lambda,\omega]}(t) - \omega c_{3,[\lambda,\omega]}(t) + \lambda c_{2,[\lambda,\omega]}(t) \\ &= \frac{1}{2} \left(\frac{\cos(\omega t - \theta_-) - (\omega - \lambda) \sin(\omega t - \theta_-)}{\sqrt{\Phi_{-,[\lambda,\omega]}}} + \frac{\cos(\omega t - \theta_+) - (\omega + \lambda) \sin(\omega t - \theta_+)}{\sqrt{\Phi_{+,[\lambda,\omega]}}} \right) \end{aligned} \quad (21)$$

$$= \frac{1}{2} \left(\frac{\sqrt{\Phi_{-,[\lambda,\omega]}} \cos(\omega t - \theta_- + \theta_-)}{\sqrt{\Phi_{-,[\lambda,\omega]}}} + \frac{\sqrt{\Phi_{+,[\lambda,\omega]}} \cos(\omega t - \theta_+ + \theta_+)}{\sqrt{\Phi_{+,[\lambda,\omega]}}} \right) \quad (22)$$

$$= \cos \omega t,$$

where Eq. (21) comes from direct substitution and Eq. (22) comes from the fact $1^2 + (\omega \pm \lambda)^2 = \Phi_{\pm,[\lambda,\omega]}$ and $a \cos t - b \sin t = \sqrt{a^2 + b^2} \cos(t + \phi)$ with $\phi = -\tan^{-1}(a/b)$, so $2a$ has

been shown. Differentiating both sides of this result respect to t using statement 1 directly yields $c_{1,[\lambda,\omega]}(t) + \omega c_{3,[\lambda,\omega]}(t) + \lambda c_{4,[\lambda,\omega]}(t) = \sin \omega t$, which is 2b. Similarly, one can also check 2c by

$$\begin{aligned}
& c_{2,[\lambda,\omega]}(t) - \omega c_{4,[\lambda,\omega]}(t) - \lambda c_{1,[\lambda,\omega]}(t) \\
&= \frac{1}{2} \left(\frac{\sin(\omega t - \theta_-) + (\omega - \lambda) \cos(\omega t - \theta_-)}{\sqrt{\Phi_{-,[\lambda,\omega]}}} - \frac{\sin(\omega t - \theta_+) + (\omega + \lambda) \cos(\omega t - \theta_+)}{\sqrt{\Phi_{+,[\lambda,\omega]}}} \right) \\
&= \frac{1}{2} \left(\frac{\sqrt{\Phi_{-,[\lambda,\omega]}} \sin(\omega t - \theta_- + \theta_-)}{\sqrt{\Phi_{-,[\lambda,\omega]}}} - \frac{\sqrt{\Phi_{+,[\lambda,\omega]}} \sin(\omega t - \theta_+ + \theta_+)}{\sqrt{\Phi_{+,[\lambda,\omega]}}} \right) \\
&= 0,
\end{aligned} \tag{23}$$

and differentiating both sides of this result respect to t using statement 1 also yields $c_{2,[\lambda,\omega]}(t) + \omega c_{4,[\lambda,\omega]}(t) - \lambda c_{3,[\lambda,\omega]}(t) = 0$, which is statement 2d. \blacksquare

Now, we can proceed to the proof of Theorem 1.

Proof. Let $\mathbf{x}^*(t)$ and \mathbf{W}^* be the corresponding periodic solution with steady synapse in Theorem 1. Let $c_{i,[\lambda,\omega]}(t)$ and $\Phi_{\pm,[\lambda,\omega]}$ be the periodic functions with parameters λ , ω and polynomials in λ defined as in Lemma B respectively. Point-blank, we propose the followings:

The solution pair $(\mathbf{x}^*(t), \mathbf{W}^*)$ are given by

$$\begin{cases} \mathbf{x}^*(t) = f(t)\mathbf{u} + g(t)\mathbf{v} \\ \mathbf{W}^* = \alpha(\mathbf{v}\mathbf{u}^\top - \mathbf{u}\mathbf{v}^\top) \end{cases} \tag{24}$$

where $\alpha \in \mathbb{R}$, and $f, g : \mathbb{R} \rightarrow \mathbb{R}$ periodic functions, and vectors \mathbf{u}, \mathbf{v} given as a form in Lemma A (i.e., $\mathbf{u} = -\Psi \sin \boldsymbol{\xi}$, $\mathbf{v} = \Psi \cos \boldsymbol{\xi}$). Especially, α , $f(t)$ and $g(t)$ are given by

$$\begin{cases} f(t) = c_{1,[\lambda_0,\omega]}(t) - \frac{\mu}{\sqrt{1-\mu^2}} c_{2,[\lambda_0,\omega]}(t) - \frac{\eta_2}{\eta_1 \sqrt{1-\mu^2}} c_{4,[\lambda_0,\omega]}(t) \\ g(t) = c_{3,[\lambda_0,\omega]}(t) + \frac{\mu}{\sqrt{1-\mu^2}} c_{4,[\lambda_0,\omega]}(t) + \frac{\eta_1}{\eta_2 \sqrt{1-\mu^2}} c_{2,[\lambda_0,\omega]}(t) \\ \alpha = \frac{\lambda_0}{\eta_1 \eta_2 \sqrt{1-\mu^2}}, \end{cases} \tag{25}$$

where λ_0 is a real root of algebraic equation $h(\lambda) = 0$ with

$$h(\lambda) = \frac{\lambda \Phi_{-,[\lambda,\omega]} \Phi_{+,[\lambda,\omega]}}{\left(\eta_1 \eta_2 \sqrt{1-\mu^2} \right) (\lambda^2 + \omega^2 + 1) + (\eta_1^2 + \eta_2^2) \omega \lambda} - \frac{\rho \sin \omega \tau}{\gamma}, \tag{26}$$

and constants η_1 , η_2 , and μ are

$$\eta_1 = \|\mathbf{u}\|, \quad \eta_2 = \|\mathbf{v}\|, \quad \text{and} \quad \mu = \frac{\mathbf{u}^\top \mathbf{v}}{\|\mathbf{u}\| \|\mathbf{v}\|}. \tag{27}$$

To begin with, we will show that the solution pair $(\mathbf{x}^*(t), \mathbf{W}^*)$ in Eq. (24) with condition (25), (26), and (27) satisfies Eq. (4). First, let's start with showing $\dot{\mathbf{x}}^* + \mathbf{x}^* - \mathbf{W}^* \mathbf{x}^* = \mathbf{b}(t)$.

According to Lemma A, such $\mathbf{b}(t)$ of form (5) is equivalent with $\cos \omega t \mathbf{u} + \sin \omega t \mathbf{v}$ on plane (see Eq. (19)) S , so it only requires checking $\dot{\mathbf{x}}^* + \mathbf{x}^* - \mathbf{W}^* \mathbf{x}^* = \cos \omega t \mathbf{u} + \sin \omega t \mathbf{v}$.

For this, from Lemma B-1, firstly see that $\dot{c}_{1, [\lambda_0, \omega]} = -\omega c_{3, [\lambda_0, \omega]}$, $\dot{c}_{2, [\lambda_0, \omega]} = -\omega c_{4, [\lambda_0, \omega]}$, $\dot{c}_{3, [\lambda_0, \omega]} = \omega c_{1, [\lambda_0, \omega]}$, and $\dot{c}_{4, [\lambda_0, \omega]} = \omega c_{2, [\lambda_0, \omega]}$. Thus from complete expression of $\mathbf{x}^*(t)$,

$$\begin{aligned} \dot{\mathbf{x}}^*(t) + \mathbf{x}^*(t) &= \left((c_1 - \omega c_3) + \frac{\mu}{\sqrt{1 - \mu^2}}(-c_2 + \omega c_4) + \frac{\eta_2}{\eta_1 \sqrt{1 - \mu^2}}(-c_2 - \omega c_4) \right) \mathbf{u} \\ &\quad + \left((c_1 + \omega c_3) + \frac{\mu}{\sqrt{1 - \mu^2}}(c_2 + \omega c_4) + \frac{\eta_1}{\eta_2 \sqrt{1 - \mu^2}}(c_2 - \omega c_4) \right) \mathbf{v}, \end{aligned} \quad (28)$$

where $_{[\lambda_0, \omega]}$ notations in $c_{i, [\lambda_0, \omega]}$ are omitted.

On the other hand, for remaining computations, we introduce some additional definitions in order to make the following processes concise. Set \mathbf{u}_\perp and \mathbf{v}_\perp as

$$\mathbf{u}_\perp = \frac{1}{\sqrt{1 - \mu^2}} \left(-\mu \mathbf{u} + \frac{\eta_1}{\eta_2} \mathbf{v} \right), \quad \mathbf{v}_\perp = \frac{1}{\sqrt{1 - \mu^2}} \left(-\frac{\eta_2}{\eta_1} \mathbf{u} + \mu \mathbf{v} \right), \quad (29)$$

where $\eta_1 = \|\mathbf{u}\|$, $\eta_2 = \|\mathbf{v}\|$ and $\mu = \mathbf{u}^\top \mathbf{v} / (\|\mathbf{u}\| \|\mathbf{v}\|)$. Then one can see that $\mathbf{u}_\perp \perp \mathbf{u}$ satisfying $\|\mathbf{u}_\perp\| = \|\mathbf{u}\|$ and $\mathbf{v}_\perp \perp \mathbf{v}$ satisfying $\|\mathbf{v}_\perp\| = \|\mathbf{v}\|$, and can further check that the expression for $\mathbf{x}^*(t)$ is equivalent with $c_{1, [\lambda_0, \omega]}(t) \mathbf{u} + c_{2, [\lambda_0, \omega]}(t) \mathbf{u}_\perp + c_{3, [\lambda_0, \omega]}(t) \mathbf{v} + c_{4, [\lambda_0, \omega]}(t) \mathbf{v}_\perp$. Now performing computation of $\mathbf{W}^* \mathbf{x}^*(t)$ yields

$$\begin{aligned} \mathbf{W}^* \mathbf{x}^*(t) &= -\lambda_0 \left(c_{2, [\lambda_0, \omega]} + \frac{\mu}{\sqrt{1 - \mu^2}} c_{1, [\lambda_0, \omega]} + \frac{\eta_2}{\eta_1 \sqrt{1 - \mu^2}} c_{3, [\lambda_0, \omega]} \right) \mathbf{u} \\ &\quad + \lambda_0 \left(-c_{4, [\lambda_0, \omega]} + \frac{\mu}{\sqrt{1 - \mu^2}} c_{3, [\lambda_0, \omega]} + \frac{\eta_1}{\eta_2 \sqrt{1 - \mu^2}} c_{1, [\lambda_0, \omega]} \right) \mathbf{v}, \end{aligned}$$

where we used the facts $\mathbf{u}^\top \mathbf{u} = \eta_1^2$, $\mathbf{v}^\top \mathbf{v} = \eta_2^2$, $\mathbf{u}^\top \mathbf{v} = \eta_1 \eta_2 \mu$, $\mathbf{u}^\top \mathbf{v}_\perp = -\eta_1 \eta_2 \sqrt{1 - \mu^2}$, and $\mathbf{v}^\top \mathbf{u}_\perp = +\eta_1 \eta_2 \sqrt{1 - \mu^2}$. Now combining above results with full notations, we have

$$\begin{aligned} &\dot{\mathbf{x}}^*(t) + \mathbf{x}^*(t) - \mathbf{W}^* \mathbf{x}^*(t) \\ &= \left((c_{1, [\lambda_0, \omega]} - \omega c_{3, [\lambda_0, \omega]} + \lambda_0 c_{2, [\lambda_0, \omega]}) - (c_{2, [\lambda_0, \omega]} - \omega c_{4, [\lambda_0, \omega]} - \lambda_0 c_{1, [\lambda_0, \omega]}) \frac{\mu}{\sqrt{1 - \mu^2}} \right. \\ &\quad \left. - (c_{2, [\lambda_0, \omega]} + \omega c_{4, [\lambda_0, \omega]} - \lambda_0 c_{3, [\lambda_0, \omega]}) \frac{\eta_2}{\eta_1 \sqrt{1 - \mu^2}} \right) \mathbf{u} \end{aligned} \quad (30)$$

$$\begin{aligned} &+ \left((c_{1, [\lambda_0, \omega]} + \omega c_{3, [\lambda_0, \omega]} + \lambda_0 c_{4, [\lambda_0, \omega]}) + (c_{2, [\lambda_0, \omega]} + \omega c_{4, [\lambda_0, \omega]} - \lambda_0 c_{3, [\lambda_0, \omega]}) \frac{\mu}{\sqrt{1 - \mu^2}} \right. \\ &\quad \left. + (c_{2, [\lambda_0, \omega]} - \omega c_{4, [\lambda_0, \omega]} - \lambda_0 c_{1, [\lambda_0, \omega]}) \frac{\eta_1}{\eta_2 \sqrt{1 - \mu^2}} \right) \mathbf{v}. \end{aligned} \quad (31)$$

Now, Lemma B-2a, 2c, and 2d tells us that each three coefficients in terms of $c_{i, [\lambda_0, \omega]}(t)$ of (30) in RHS is $\cos \omega t$, 0, and 0 respectively, thus simplified only into $\cos \omega t \mathbf{u}$. Similarly, each three coefficients in terms of $c_{i, [\lambda_0, \omega]}(t)$ in (31) becomes $\sin \omega t$, 0, and 0 by Lemma B-2b, 2c, and 2d respectively, thus yielding $\sin \omega t \mathbf{v}$. Therefore in total, completing the proof of $\dot{\mathbf{x}}^*(t) + \mathbf{x}^*(t) - \mathbf{W}^* \mathbf{x}^*(t) = \cos \omega t \mathbf{u} + \sin \omega t \mathbf{v} = \mathbf{b}(t)$.

Now, it remains to confirm $-\gamma \mathbf{W}^* + \rho(\mathbf{x}^* \mathbf{x}_\tau^{*\top} - \mathbf{x}_\tau^* \mathbf{x}^{*\top}) = \mathbf{O}$. In order to show this, first we have to compute the term $\mathbf{x}^* \mathbf{x}_\tau^{*\top} - \mathbf{x}_\tau^* \mathbf{x}^{*\top}$. Putting $\mathbf{x}(t) = c_{1, [\lambda_0, \omega]}(t) \mathbf{u} + c_{2, [\lambda_0, \omega]}(t) \mathbf{u}_\perp +$

$c_{3,[\lambda_0,\omega]}(t)\mathbf{v} + c_{4,[\lambda_0,\omega]}(t)\mathbf{v}_\perp$ and doing some lengthy computations with the help of following trigonometric relations

$$\begin{cases} \cos(\omega t - \theta_-) \sin(\omega t - \theta_+)_\tau - \cos(\omega t - \theta_-)_\tau \sin(\omega t - \theta_+) = -\sin \omega \tau \cos(\theta_- - \theta_+) \\ \sin(\omega t - \theta_-) \sin(\omega t - \theta_+)_\tau - \sin(\omega t - \theta_-)_\tau \sin(\omega t - \theta_+) = \sin \omega \tau \sin(\theta_- - \theta_+) \\ \sin(\omega t - \theta_-) \cos(\omega t - \theta_+)_\tau - \sin(\omega t - \theta_-)_\tau \cos(\omega t - \theta_+) = \sin \omega \tau \cos(\theta_- - \theta_+) \\ \cos(\omega t - \theta_-) \cos(\omega t - \theta_+)_\tau - \cos(\omega t - \theta_-)_\tau \cos(\omega t - \theta_+) = \sin \omega \tau \sin(\theta_- - \theta_+), \end{cases} \quad (32)$$

then one gets

$$\begin{aligned} & \mathbf{x}^*(t)\mathbf{x}^*(t-\tau)^\top - \mathbf{x}^*(t-\tau)\mathbf{x}^*(t)^\top \\ &= \frac{\sin \omega \tau}{4} \left[\left(\frac{1}{\Phi_{-,[\lambda_0,\omega]}} - \frac{1}{\Phi_{+,[\lambda_0,\omega]}} \right) ((\mathbf{u}_\perp \mathbf{u}^\top - \mathbf{u} \mathbf{u}_\perp^\top) + (\mathbf{v}_\perp \mathbf{v}^\top - \mathbf{v} \mathbf{v}_\perp^\top)) \right. \\ & \quad + \left(\frac{1}{\Phi_{-,[\lambda_0,\omega]}} + \frac{1}{\Phi_{+,[\lambda_0,\omega]}} + \frac{2 \cos(\theta_{-,[\lambda_0,\omega]} - \theta_{+,[\lambda_0,\omega]})}{\Phi_{-,[\lambda_0,\omega]} \Phi_{+,[\lambda_0,\omega]}} \right) (\mathbf{v} \mathbf{u}^\top - \mathbf{u} \mathbf{v}^\top) \\ & \quad + \left(\frac{1}{\Phi_{-,[\lambda_0,\omega]}} + \frac{1}{\Phi_{+,[\lambda_0,\omega]}} - \frac{2 \cos(\theta_{-,[\lambda_0,\omega]} - \theta_{+,[\lambda_0,\omega]})}{\Phi_{-,[\lambda_0,\omega]} \Phi_{+,[\lambda_0,\omega]}} \right) (\mathbf{v}_\perp \mathbf{u}_\perp^\top - \mathbf{u}_\perp \mathbf{v}_\perp^\top) \\ & \quad \left. + \frac{2 \sin(\theta_{-,[\lambda_0,\omega]} - \theta_{+,[\lambda_0,\omega]})}{\Phi_{-,[\lambda_0,\omega]} \Phi_{+,[\lambda_0,\omega]}} ((\mathbf{v}_\perp \mathbf{u}^\top - \mathbf{u} \mathbf{v}_\perp^\top) + (\mathbf{v} \mathbf{u}_\perp^\top - \mathbf{u}_\perp \mathbf{v}^\top)) \right], \quad (33) \end{aligned}$$

which is a constant in t as expected. Here, from (29), one can easily check that the six anti-symmetric matrix terms in (33) satisfy the following relations:

$$\begin{cases} \mathbf{u}_\perp \mathbf{u}^\top - \mathbf{u} \mathbf{u}_\perp^\top = \frac{\eta_1}{\eta_2 \sqrt{1 - \mu^2}} (\mathbf{v} \mathbf{u}^\top - \mathbf{u} \mathbf{v}^\top) \\ \mathbf{v}_\perp \mathbf{v}^\top - \mathbf{v} \mathbf{v}_\perp^\top = \frac{\eta_2}{\eta_1 \sqrt{1 - \mu^2}} (\mathbf{v} \mathbf{u}^\top - \mathbf{u} \mathbf{v}^\top) \\ \mathbf{v}_\perp \mathbf{u}_\perp^\top - \mathbf{u}_\perp \mathbf{v}_\perp^\top = \mathbf{v} \mathbf{u}^\top - \mathbf{u} \mathbf{v}^\top \\ \mathbf{v} \mathbf{u}_\perp^\top - \mathbf{u}_\perp \mathbf{v}^\top = -(\mathbf{v}_\perp \mathbf{u}^\top - \mathbf{u} \mathbf{v}_\perp^\top). \end{cases} \quad (34)$$

Now simplifying (33) using (34) in terms of $\mathbf{v} \mathbf{u}^\top - \mathbf{u} \mathbf{v}^\top$ and substituting the result into $-\gamma \mathbf{W}^* + \rho(\mathbf{x}^* \mathbf{x}_\tau^{*\top} - \mathbf{x}_\tau^* \mathbf{x}^{*\top})$ alongside substituting $\mathbf{W}^* = \lambda_0(\mathbf{v} \mathbf{u}^\top - \mathbf{u} \mathbf{v}^\top) / (\eta_1 \eta_2 \sqrt{1 - \mu^2})$ together, then

$$\begin{aligned} & -\gamma \mathbf{W}^* + \rho(\mathbf{x}^* \mathbf{x}_\tau^{*\top} - \mathbf{x}_\tau^* \mathbf{x}^{*\top}) \quad (35) \\ &= \left[-\frac{\gamma \lambda_0}{\eta_1 \eta_2 \sqrt{1 - \mu^2}} + \frac{\rho \sin \omega \tau}{\Phi_{-,[\lambda_0,\omega]} \Phi_{+,[\lambda_0,\omega]}} \left(\lambda_0^2 + \frac{(\eta_1^2 + \eta_2^2) \omega}{\eta_1 \eta_2 \sqrt{1 - \mu^2}} \lambda_0 + \omega^2 + 1 \right) \right] (\mathbf{v} \mathbf{u}^\top - \mathbf{u} \mathbf{v}^\top). \end{aligned}$$

Moreover, from the fact that λ_0 is a root of (26), we know

$$\frac{\lambda_0 \Phi_{-,[\lambda_0,\omega]} \Phi_{+,[\lambda_0,\omega]}}{(\eta_1 \eta_2 \sqrt{1 - \mu^2}) (\lambda_0^2 + \omega^2 + 1) + (\eta_1^2 + \eta_2^2) \omega \lambda_0} - \frac{\rho \sin \omega \tau}{\gamma} = 0, \quad (36)$$

and slight more algebra using this shows that the large-bracketed term in (35) turns out to be 0, so proving $-\gamma \mathbf{W}^* + \rho(\mathbf{x}^* \mathbf{x}_\tau^{*\top} - \mathbf{x}_\tau^* \mathbf{x}^{*\top}) = \mathbf{O}$.

From all above, we conclude that Eq. (24) with conditions (25), (26), and (27) is a solution of Eq. (4). ■

B3: Proof of Theorem 2 and the Retrievability Conditions

Since Eq. (6) is a perturbed linear ordinary differential equation, we can obtain explicit solution of $\mathbf{x}_r(t)$ using the variational formula, i.e.,

$$\begin{aligned}\mathbf{x}_r(t) &= e^{t(\mathbf{W}^* - \mathbf{I})} \mathbf{x}_r(0) + \int_0^t e^{s(\mathbf{W}^* - \mathbf{I})} \sin(\omega(t-s)) \mathbf{m}_c \, ds \\ &= e^{-t} e^{t\mathbf{W}^*} \mathbf{x}_r(0) + \int_0^t e^{-s} \sin(\omega(t-s)) e^{s\mathbf{W}^*} \mathbf{m}_c \, ds.\end{aligned}\quad (37)$$

Here, from the fact that $e^{t\mathbf{W}^*} \mathbf{x}_0$ is a flow generated by $\dot{\mathbf{x}} = \mathbf{W}^* \mathbf{x}$, $\mathbf{x}(0) = \mathbf{x}_0$, any non-trivial $\mathbf{x}_0 \in S = \text{Span}\{\mathbf{u}, \mathbf{v}\}$ will generate purely rotational flow on S since $\mathbf{W}^* = \alpha(\mathbf{v}\mathbf{u}^\top - \mathbf{u}\mathbf{v}^\top) \in \wedge^2(S)$ is rank-2 anti-symmetric. More specifically, there is some $\mathbf{x}_{0\wedge} \in S$ perpendicular to \mathbf{x}_0 with $\|\mathbf{x}_{0\wedge}\| = \|\mathbf{x}_0\|$, so that

$$e^{t\mathbf{W}^*} \mathbf{x}_0 = \cos \lambda^* t \mathbf{x}_0 + \sin \lambda^* t \mathbf{x}_{0\wedge} \quad (38)$$

where λ^* being the magnitude of only imaginary eigenvalue (which is in pair) of \mathbf{W}^* . This gives us an idea of decomposing \mathbf{m}_c into $\mathbf{m}_c = \bar{\mathbf{m}}_c + \tilde{\mathbf{m}}_c$ where $\bar{\mathbf{m}}_c = \text{Proj}_S \mathbf{m}_c$ (so that $\|\tilde{\mathbf{m}}_c\| = \text{Dist}(\mathbf{m}_c, S)$, and $\tilde{\mathbf{m}}_c \perp S$), then RHS of Eq. (37) is decomposed into

$$\begin{aligned}\mathbf{x}_r(t) &= e^{-t} e^{t\mathbf{W}^*} \mathbf{x}_r(0) + \int_0^t e^{-s} \sin(\omega(t-s)) \tilde{\mathbf{m}}_c \, ds \\ &\quad + \int_0^t e^{-s} (\cos(\lambda^* s) \sin(\omega(t-s)) \bar{\mathbf{m}}_c + \sin(\lambda^* s) \sin(\omega(t-s)) \bar{\mathbf{m}}_{c\wedge}) \, ds,\end{aligned}\quad (39)$$

where $\bar{\mathbf{m}}_{c\wedge}$ is decided by $\bar{\mathbf{m}}_c$ in the means of relationship between $\mathbf{x}_{0\wedge}$ and \mathbf{x}_0 in Eq. (38).

Computing the asymptotic behaviour of each integral as $t \rightarrow \infty$ and using the fact that the term $e^{-t} e^{t\mathbf{W}^*} \mathbf{x}_r(0)$ decays to $\mathbf{0}$ as $t \rightarrow \infty$, then Eq. (39) turns out to be asymptotically approaching the following periodic function

$$\boxed{\mathbf{x}_r^*(t) = \frac{1}{\sqrt{\omega^2 + 1}} \sin(\omega t - \theta) \tilde{\mathbf{m}}_c + c_{3, [\lambda^*, \omega]}(t) \bar{\mathbf{m}}_c + c_{4, [\lambda^*, \omega]}(t) \bar{\mathbf{m}}_{c\wedge},} \quad (40)$$

where $\theta = \tan^{-1} \omega$, and periodic functions $c_{3, [\lambda^*, \omega]}(t)$, $c_{4, [\lambda^*, \omega]}(t)$ are from Lemma B with parameters λ^* and ω .

This $\mathbf{x}_r^*(t)$ is also a solution of Eq. (6). To show this, directly substituting Eq. (40) into Eq. (6) and simplifying by collecting the terms of each $\tilde{\mathbf{m}}_c$, $\bar{\mathbf{m}}_c$, and $\bar{\mathbf{m}}_{c\wedge}$, then one can verify that

$$\begin{aligned}&\left(\frac{\omega}{\sqrt{\omega^2 + 1}} \cos(\omega t - \theta) + \frac{1}{\sqrt{\omega^2 + 1}} \sin(\omega t - \theta) \right) \tilde{\mathbf{m}}_c \\ &\quad + (c_{1, [\lambda^*, \omega]}(t) + \omega c_{3, [\lambda^*, \omega]}(t) + \lambda^* c_{4, [\lambda^*, \omega]}(t)) \bar{\mathbf{m}}_c \\ &\quad + (c_{2, [\lambda^*, \omega]}(t) + \omega c_{4, [\lambda^*, \omega]}(t) - \lambda^* c_{3, [\lambda^*, \omega]}(t)) \bar{\mathbf{m}}_{c\wedge} - \sin \omega t \mathbf{m}_c = \mathbf{0},\end{aligned}\quad (41)$$

where each $c_{1, [\lambda^*, \omega]}(t)$, $c_{2, [\lambda^*, \omega]}(t)$ arises from the differentiation of $c_{3, [\lambda^*, \omega]}(t)$ and $c_{4, [\lambda^*, \omega]}(t)$ with respect to t as in Lemma B-1, and the alternate representation of $\mathbf{W}^* \in \wedge^2(S)$ with $\mathbf{W}^* = \alpha(\mathbf{v}\mathbf{u}^\top - \mathbf{u}\mathbf{v}^\top) = \frac{\lambda^*}{\nu^2} (\bar{\mathbf{m}}_c \bar{\mathbf{m}}_{c\wedge}^\top - \bar{\mathbf{m}}_{c\wedge} \bar{\mathbf{m}}_c^\top)$ where $\nu = \|\bar{\mathbf{m}}_c\|$ has been used.

If one can show the equivalence of the LHS with $\mathbf{0}$, then it is done. In the LHS, the coefficient of $\tilde{\mathbf{m}}_c$ is directly $\sin \omega t$, and the coefficient of $\bar{\mathbf{m}}_c$ is also equivalent to $\sin \omega t$ by Lemma B-2b. On the other hand, the coefficient of $\bar{\mathbf{m}}_{c\wedge}$ is 0 by Lemma B-2d. Thus the LHS

is actually $\sin \omega t (\tilde{\mathbf{m}}_c + \bar{\mathbf{m}}_c) - \sin \omega t \mathbf{m}_c$, which simply $\mathbf{0}$. This proves that the converging limit-cycle orbit $\mathbf{x}_r^*(t)$ of $\mathbf{x}_r(t)$ is also a solution of Eq. (6).

To show the remaining statements, let \mathcal{M} be the retrievable subspace with respect to a representation set $\{\mathbf{m}_i\}_{i=1}^n$, and consider the case that $\mathbf{m}_c \notin S_\perp$. Then $\bar{\mathbf{m}}_c, \bar{\mathbf{m}}_{c\wedge} \neq \mathbf{0}$, and since $\bar{\mathbf{m}}_c, \bar{\mathbf{m}}_{c\wedge} \in S = \text{Span}\{\mathbf{u}, \mathbf{v}\}$, one can directly see that also $\bar{\mathbf{m}}_c, \bar{\mathbf{m}}_{c\wedge} \in \mathcal{M} \setminus \{\mathbf{0}\}$. Now, we claim that the term $c_{3, [\lambda^*, \omega]}(t) \bar{\mathbf{m}}_c + c_{4, [\lambda^*, \omega]}(t) \bar{\mathbf{m}}_{c\wedge}$ in Eq. (40) always lies in $\mathcal{M} \setminus \{\mathbf{0}\}$. This can be shown from the following alternate expressions of $c_{3, [\lambda^*, \omega]}(t)$ and $c_{4, [\lambda^*, \omega]}(t)$:

$$c_{3, [\lambda^*, \omega]}(t) = \sqrt{\alpha^2 + \beta^2} \sin(\omega t + \Delta_1) \quad \text{and} \quad c_{4, [\lambda^*, \omega]}(t) = \sqrt{\alpha^2 + \beta^2} \sin(\omega t + \Delta_2), \quad (42)$$

$$\text{where} \quad \begin{cases} \alpha = \frac{1}{2} \left(\frac{\cos \theta_{-, [\lambda^*, \omega]}}{\sqrt{\Phi_{-, [\lambda^*, \omega]}}} + \frac{\cos \theta_{+, [\lambda^*, \omega]}}{\sqrt{\Phi_{+, [\lambda^*, \omega]}}} \right) \\ \beta = \frac{1}{2} \left(\frac{\sin \theta_{-, [\lambda^*, \omega]}}{\sqrt{\Phi_{-, [\lambda^*, \omega]}}} + \frac{\sin \theta_{+, [\lambda^*, \omega]}}{\sqrt{\Phi_{+, [\lambda^*, \omega]}}} \right) \end{cases} \quad \text{and} \quad \begin{cases} \Delta_1 = \tan^{-1} \left(-\frac{\beta}{\alpha} \right) \\ \Delta_2 = \tan^{-1} \left(\frac{\alpha}{\beta} \right). \end{cases} \quad (43)$$

From Eq. (42), one can read that the only condition making $c_{3, [\lambda^*, \omega]}$ and $c_{4, [\lambda^*, \omega]}$ to vanish simultaneously is $\Delta_1 = \Delta_2$, and the bijective property of the arctangent function implies

$$-\frac{\beta}{\alpha} = \frac{\alpha}{\beta} \quad \iff \quad \alpha^2 + \beta^2 = 0, \quad (44)$$

thus yielding $\alpha = \beta = 0$, which only is a pointless triviality.

From this, one can assure that $\mathbf{x}_r^*(t)$ must belongs to $\mathcal{M} \setminus \{\mathbf{0}\}$ on instances that making the coefficient of $\tilde{\mathbf{m}}_c$ in Eq. (40) to vanish. Denoting such time t as $t = t^\dagger$, we derive that such t^\dagger must satisfy $\omega t^\dagger - \theta = n\pi$, $n \in \mathbb{Z}$, that is,

$$\boxed{t^\dagger = \frac{1}{\omega} \tan^{-1} \omega + n \frac{\pi}{\omega}, \quad n \in \mathbb{Z}, \quad (t^\dagger > 0),} \quad (45)$$

which yields Eq. (11) indicating periodic retrieval. This proves that $\mathbf{x}_r^*(t)$ with $t = t^\dagger$ is always retrievable unless $\mathbf{m}_c \notin S_\perp$. Besides, if $\mathbf{m}_c \in \mathcal{M}$, then one can easily see $\tilde{\mathbf{m}}_c \in \mathcal{M}$ thus $\mathbf{x}_r^*(t) \in \mathcal{M} \setminus \{\mathbf{0}\}$ for all t , so always being retrievable.

On the other hand, considering the case when $\mathbf{m}_c \in S_\perp$, first suppose that also $\mathbf{m}_c \in \mathcal{M}$. Then, $\bar{\mathbf{m}}_c, \bar{\mathbf{m}}_{c\wedge} = \mathbf{0}$, but $\tilde{\mathbf{m}}_c \neq \mathbf{0}$. Thus $\mathbf{x}_r^*(t) \in \mathcal{M}$ for all t , but especially only on $t = t^\dagger$, $\mathbf{x}_r^*(t) = \mathbf{0}$. In contrary, if $\mathbf{m}_c \notin \mathcal{M}$, then also $\bar{\mathbf{m}}_c, \bar{\mathbf{m}}_{c\wedge} = \mathbf{0}$, and even $\tilde{\mathbf{m}}_c \notin \mathcal{M}$, therefore $\mathbf{x}_r^*(t) \notin \mathcal{M} \setminus \{\mathbf{0}\}$ for all t , so never becoming retrievable.

Summing up above results, the retrievability conditions in main text page 6 and Theorem 2 have been proved. \blacksquare

B4: Proof of Theorem 3

One can directly use $\cos \theta_i = \frac{\|\text{Proj}_S(\xi_1, \dots, \xi_n) \mathbf{m}_i\|}{\|\mathbf{m}_i\|}$ where $S(\xi_1, \dots, \xi_n)$ denotes the memory plane determined with the choice of $\{\xi_i\}_{i=1}^n$. Firstly, one can generally observe that for any $\mathbf{m} \in \mathbb{R}^N$ and $S = \text{Span}\{\mathbf{u}, \mathbf{v}\}$,

$$\text{Proj}_S \mathbf{m} = \text{Proj}_{\text{Span}\{\mathbf{u}, \mathbf{v}\}} \mathbf{m} = \frac{\mathbf{m}^\top \mathbf{u}}{\|\mathbf{u}\|} \mathbf{u} + \frac{\mathbf{m}^\top \mathbf{u}_\perp}{\|\mathbf{u}_\perp\|} \mathbf{u}_\perp, \quad (46)$$

where $\mathbf{u}_\perp \in \text{Span}\{\mathbf{u}, \mathbf{v}\}$ satisfying $\mathbf{u}_\perp \perp \mathbf{u}$ and $\|\mathbf{u}_\perp\| = \|\mathbf{u}\|$, in which can be specifically expressed as in Eq. (29). Thus substituting it into above equation yields

$$\text{Proj}_S \mathbf{m}_i = \frac{1}{1 - \mu^2} \left(\frac{\mathbf{m}_i^\top \mathbf{u}}{\eta_1^2} - \mu \frac{\mathbf{m}_i^\top \mathbf{v}}{\eta_1 \eta_2} \right) \mathbf{u} + \frac{1}{1 - \mu^2} \left(\frac{\mathbf{m}_i^\top \mathbf{v}}{\eta_2^2} - \mu \frac{\mathbf{m}_i^\top \mathbf{u}}{\eta_1 \eta_2} \right) \mathbf{v}, \quad (47)$$

where $\eta_1 = \|\mathbf{u}\|$, $\eta_2 = \|\mathbf{v}\|$ and $\mu = \mathbf{u}^\top \mathbf{v} / (\|\mathbf{u}\| \|\mathbf{v}\|)$. Besides, from the fact

$$\|\text{Proj}_S \mathbf{m}_i\|^2 = \mathbf{m}_i \cdot \text{Proj}_S \mathbf{m}_i, \quad (48)$$

for \mathbf{u}, \mathbf{v} defined as in Lemma A, one can directly read that

$$\|\text{Proj}_{S(\xi_1, \dots, \xi_n)} \mathbf{m}_i\| = \sqrt{\frac{\left(\frac{\mathbf{m}_i^\top \mathbf{u}}{\eta_1}\right)^2 + \left(\frac{\mathbf{m}_i^\top \mathbf{v}}{\eta_2}\right)^2 - 2\mu \frac{(\mathbf{m}_i^\top \mathbf{u})(\mathbf{m}_i^\top \mathbf{v})}{\eta_1 \eta_2}}{1 - \mu^2}}. \quad (49)$$

Let $\|\mathbf{m}_i\| = l$. Since $\mathbf{u} = -\Psi \sin \boldsymbol{\xi} = \sum_{i=1}^n \sin \xi_i \mathbf{m}_i$, and $\mathbf{v} = \Psi \cos \boldsymbol{\xi} = \sum_{i=1}^n \cos \xi_i \mathbf{m}_i$, the orthogonality of $\{\mathbf{m}_i\}_{i=1}^n$ guarantees $\mathbf{m}_i^\top \mathbf{u} = -\sin \xi_i$, and $\mathbf{m}_i^\top \mathbf{v} = \cos \xi_i$. Further, one can easily verify that

$$\eta_1 = l^2 \sum_{j=1}^n \sin^2 \xi_j, \quad \eta_2 = l^2 \sum_{j=1}^n \cos^2 \xi_j \quad \text{and} \quad \mu = -\frac{\sum_{j=1}^n \sin \xi_j \cos \xi_j}{\sqrt{\left(\sum_{j=1}^n \sin^2 \xi_j\right) \left(\sum_{j=1}^n \cos^2 \xi_j\right)}},$$

so substituting these expressions into Eq. (49) and completing tedious simplification procedure, we finally deduce

$$\frac{\|\text{Proj}_{S(\xi_1, \dots, \xi_n)} \mathbf{m}_i\|}{\|\mathbf{m}_i\|} = \sqrt{\frac{\sum_{j=1}^n \sin^2(\xi_j - \xi_i)}{\sum_{\substack{j,k=1 \\ j>k}}^n \sin^2(\xi_j - \xi_k)}}. \quad (50)$$

Note that this value does not depend on $l = \|\mathbf{m}_i\|$. Now, consider the following double summation $\sum_{i,j=1}^n \sin^2(\xi_j - \xi_i)$. This is exactly the sum with respect to i performed to the squared numerator of the last term in Eq. (50). Moreover, $\sin^2(\xi_j - \xi_i) = \sin^2(\xi_i - \xi_j)$ and is zero when $j = i$, thus we read that

$$\sum_{i,j=1}^n \sin^2(\xi_j - \xi_i) = 2 \sum_{\substack{i,j=1 \\ j>i}}^n \sin^2(\xi_j - \xi_i), \quad (51)$$

which the term $\sum_{\substack{i,j=1 \\ j>i}}^n \sin^2(\xi_j - \xi_i)$ is identical the squared denominator of the last term in Eq. (50). This directly leads to the following strong result:

$$\boxed{\sum_{i=1}^n \left(\frac{\|\text{Proj}_{S(\xi_1, \dots, \xi_n)} \mathbf{m}_i\|}{\|\mathbf{m}_i\|} \right)^2 = 2}. \quad (52)$$

From this, we see that by the Cauchy-Schwarz inequality, the maximum of $\langle \cos \theta_i \rangle_i = \frac{1}{n} \sum_{i=1}^n \frac{\|\text{Proj}_{S(\xi_1, \dots, \xi_n)} \mathbf{m}_i\|}{\|\mathbf{m}_i\|}$ is achieved with value $\sqrt{\frac{2}{n}}$ when each $\cos \theta_i = \frac{\|\text{Proj}_{S(\xi_1, \dots, \xi_n)} \mathbf{m}_i\|}{\|\mathbf{m}_i\|} = \frac{\sqrt{2n}}{n} = \sqrt{\frac{2}{n}}$ for all $i = 1, \dots, n$, so proving Eq. (12).

However, finding the possible distributions of ξ_i achieving the maximum is quite difficult, but we claim that such distribution exists, and one family of those are given as in (12). To show this, first suppose that each ξ_i is chosen as (12) but with zero shifts, i.e.,

$\alpha = 0$, and denote such values with $\bar{\xi}_i$. We first verify that $\mathbf{u} \perp \mathbf{v}$ in this case. Observe that when n is even,

$$\begin{aligned}
\mathbf{u}^\top \mathbf{v} &= - \sum_{i=1}^n \sin \bar{\xi}_i \cos \bar{\xi}_i = - \sin \bar{\xi}_1 \cos \bar{\xi}_1 - \sum_{i=2}^n \sin \bar{\xi}_i \cos \bar{\xi}_i \\
&= 0 - \sum_{i=2}^{n/2} (\sin \bar{\xi}_i \cos \bar{\xi}_i + \sin \bar{\xi}_{n-i+2} \cos \bar{\xi}_{n-i+2}) + \sin \bar{\xi}_{n/2+1} \cos \bar{\xi}_{n/2+1} \\
&= - \sum_{i=2}^{n/2} (\sin \bar{\xi}_i \cos \bar{\xi}_i + \sin(\pi - \bar{\xi}_i) \cos(\pi - \bar{\xi}_i)) + \sin \frac{\pi}{2} \cos \frac{\pi}{2} = 0, \tag{53}
\end{aligned}$$

and similarly when n is odd,

$$\begin{aligned}
\mathbf{u}^\top \mathbf{v} &= - \sum_{i=1}^n \sin \bar{\xi}_i \cos \bar{\xi}_i \\
&= - \sin \bar{\xi}_1 \cos \bar{\xi}_1 - \sum_{i=2}^{(n+1)/2} (\sin \bar{\xi}_i \cos \bar{\xi}_i + \sin \bar{\xi}_{n-i+2} \cos \bar{\xi}_{n-i+2}) \\
&= 0 - \sum_{i=2}^{(n+1)/2} (\sin \bar{\xi}_i \cos \bar{\xi}_i + \sin(\pi - \bar{\xi}_i) \cos(\pi - \bar{\xi}_i)) = 0. \tag{54}
\end{aligned}$$

Therefore, $\mathbf{u} \perp \mathbf{v}$, so simply considering a $\mu = 0$ case in Eq. (49), we have

$$\frac{\|\text{Proj}_{S(\bar{\xi}_1, \dots, \bar{\xi}_n)} \mathbf{m}_i\|}{\|\mathbf{m}_i\|} = \sqrt{\frac{\sin^2 \bar{\xi}_i}{\sum_{j=1}^n \sin^2 \bar{\xi}_j} + \frac{\cos^2 \bar{\xi}_i}{\sum_{j=1}^n \cos^2 \bar{\xi}_j}}, \quad i = 1, \dots, n. \tag{55}$$

Here, one can even show that

$$\sum_{j=1}^n \sin^2 \bar{\xi}_j = \sum_{j=1}^n \cos^2 \bar{\xi}_j = \frac{n}{2} \tag{56}$$

by observing the following: From Riemann integral,

$$\Delta \sum_{j=1}^n \sin^2 \bar{\xi}_j \approx \int_0^\pi \sin^2 \theta \, d\theta = \frac{\pi}{2}, \quad \Delta \sum_{j=1}^n \cos^2 \bar{\xi}_j \approx \int_0^\pi \cos^2 \theta \, d\theta = \frac{\pi}{2} \tag{57}$$

as $n \rightarrow \infty$ where $\Delta = \pi/n$ being the interval between each sampling points $\bar{\xi}_j$. However, by the symmetry of functions $\cos^2 \theta$ and $\sin^2 \theta$ on interval $[0, \pi]$ and the arithmetically sequenced property of $\bar{\xi}_j$, one can luckily confirm that the approximation (57) is actually an equality for all n . Thus we finally have

$$\sum_{j=1}^n \sin^2 \bar{\xi}_j = \sum_{j=1}^n \cos^2 \bar{\xi}_j = \frac{\pi}{2\Delta} = \frac{\pi}{2 \cdot \frac{\pi}{n}}, \tag{58}$$

which yields Eq. (56). Therefore, we can now write Eq. (55) simply as

$$\frac{\|\text{Proj}_{S(\bar{\xi}_1, \dots, \bar{\xi}_n)} \mathbf{m}_i\|}{\|\mathbf{m}_i\|} = \sqrt{\frac{2(\sin^2 \bar{\xi}_i + \cos^2 \bar{\xi}_i)}{n}} = \sqrt{\frac{2}{n}}, \quad i = 1, \dots, n. \tag{59}$$

This indicates that the value of $\|\text{Proj}_{S(\bar{\xi}_1, \dots, \bar{\xi}_n)} \mathbf{m}_i\|$ is constant throughout every $i = 1, \dots, n$ with value $\sqrt{2/n}$, so such set of $\{\bar{\xi}_i\}_{i=1}^n$ (i.e., in Eq. (12) with $\alpha = 0$) can achieve $\max_{\xi_1, \dots, \xi_n} \frac{\|\text{Proj}_{S(\xi_1, \dots, \xi_n)} \mathbf{m}_i\|}{\|\mathbf{m}_i\|} = \sqrt{2/n}$.

Lastly, for the remaining $\alpha \neq 0$ case, i.e., $0 < \alpha < \frac{\pi}{n}$, recall that $\xi_i^* = \bar{\xi}_i + \alpha$. Let's denote $\mathbf{b}_{(\xi_1, \dots, \xi_n)}(t) = \sum_{i=1}^n \sin(\omega t - \xi_i) \mathbf{m}_i$ as the input orbit generated by $\{\xi_i\}_{i=1}^n$. Then, one can easily see that $\mathbf{b}_{(\xi_1^*, \dots, \xi_n^*)}(t) = \mathbf{b}_{(\bar{\xi}_1, \dots, \bar{\xi}_n)}(t + \frac{\alpha}{\omega})$ for any t , so the orbit of $\mathbf{b}_{(\xi_1^*, \dots, \xi_n^*)}$ and $\mathbf{b}_{(\bar{\xi}_1, \dots, \bar{\xi}_n)}$ is actually identical thus sharing the same plane, i.e., $S(\xi_1^*, \dots, \xi_n^*) \equiv S(\bar{\xi}_1, \dots, \bar{\xi}_n)$ from Lemma A. Thus, one must have $\langle \cos \theta_i(\xi_1^*, \dots, \xi_n^*) \rangle_i = \langle \cos \theta_i(\bar{\xi}_1, \dots, \bar{\xi}_n) \rangle_i = \sqrt{\frac{2}{n}}$, which implies that $\xi_i^* = \bar{\xi}_i + \alpha = \frac{\pi}{n}(i-1) + \alpha$ also achieves the maximum of $\langle \cos \theta_i \rangle_i$. ■

Appendix C: Stability Analysis of the Periodic Solution $(\mathbf{x}^*(t), \mathbf{W}^*)$

C1: Derivation of the Variational Equation, Eq. (10)

First, rewriting the original system (4) into a general form, then

$$\begin{cases} \dot{\mathbf{x}} = \mathbf{f}(\mathbf{x}, \mathbf{W}) \\ \dot{\mathbf{W}} = \mathbf{G}(\mathbf{x}, \mathbf{x}_\tau, \mathbf{W}) \end{cases} \text{ where } \begin{cases} \mathbf{f}(\mathbf{x}, \mathbf{W}) = -\mathbf{x} + \mathbf{W}\mathbf{x} + \mathbf{b}(t), \\ \mathbf{G}(\mathbf{x}, \mathbf{x}_\tau, \mathbf{W}) = -\gamma \mathbf{W} + \rho (\mathbf{x}\mathbf{x}_\tau^\top - \mathbf{x}_\tau \mathbf{x}^\top). \end{cases} \quad (60)$$

Considering deviation $\mathbf{x}(t) = \mathbf{x}^*(t) + \delta \mathbf{x}(t)$ and $\mathbf{W}(t) = \mathbf{W}^* + \delta \mathbf{W}(t)$ from reference trajectory $(\mathbf{x}^*, \mathbf{W}^*)$, we have

$$\begin{cases} \dot{\mathbf{x}}^* + \delta \dot{\mathbf{x}} = \mathbf{f}(\mathbf{x}^* + \delta \mathbf{x}, \mathbf{W}^* + \delta \mathbf{W}) \\ \dot{\mathbf{W}}^* + \delta \dot{\mathbf{W}} = \mathbf{G}(\mathbf{x}^* + \delta \mathbf{x}, \mathbf{x}_\tau^* + \delta \mathbf{x}_\tau, \mathbf{W}^* + \delta \mathbf{W}). \end{cases} \quad (61)$$

Now, applying first-ordered Taylor expansion on $(\mathbf{x}^*, \mathbf{W}^*)$ to each RHS and using $\dot{\mathbf{x}}^* = \mathbf{f}(\mathbf{x}^*, \mathbf{W}^*)$ and $\dot{\mathbf{W}}^* = \mathbf{G}(\mathbf{x}^*, \mathbf{x}_\tau^*, \mathbf{W}^*) = \mathbf{O}$, we get

$$\begin{cases} \delta \dot{\mathbf{x}} = \frac{\partial \mathbf{f}}{\partial \mathbf{x}} \Big|_{(\mathbf{x}^*, \mathbf{W}^*)} \cdot \delta \mathbf{x} + \frac{\partial \mathbf{f}}{\partial \mathbf{W}} \Big|_{(\mathbf{x}^*, \mathbf{W}^*)} : \delta \mathbf{W} \\ \delta \dot{\mathbf{W}} = \frac{\partial \mathbf{G}}{\partial \mathbf{x}} \Big|_{(\mathbf{x}^*, \mathbf{x}_\tau^*, \mathbf{W}^*)} \cdot \delta \mathbf{x} + \frac{\partial \mathbf{G}}{\partial \mathbf{x}_\tau} \Big|_{(\mathbf{x}^*, \mathbf{x}_\tau^*, \mathbf{W}^*)} \cdot \delta \mathbf{x}_\tau + \frac{\partial \mathbf{G}}{\partial \mathbf{W}} \Big|_{(\mathbf{x}^*, \mathbf{x}_\tau^*, \mathbf{W}^*)} : \delta \mathbf{W}, \end{cases} \quad (62)$$

where $:$ is used for the *double dot product* notation. Now computing each tensor-represented Jacobians, firstly we immediately see $\frac{\partial \mathbf{f}}{\partial \mathbf{x}} = -\mathbf{I} + \mathbf{W}$, therefore

$$\frac{\partial \mathbf{f}}{\partial \mathbf{x}} \Big|_{(\mathbf{x}^*, \mathbf{W}^*)} \cdot \delta \mathbf{x} = (-\mathbf{I} + \mathbf{W}^*) \delta \mathbf{x}. \quad (63)$$

For the remaining ones, observe that $\frac{\partial \mathbf{f}}{\partial \mathbf{W}}$ is a third-order tensor and each element can be found by

$$\begin{aligned} \left(\frac{\partial \mathbf{f}}{\partial \mathbf{W}} \right)_{ijk} &= \frac{\partial f_i}{\partial W_{jk}} = \frac{\partial}{\partial W_{jk}} \left(-x_i + \sum_l W_{il} x_l + b_i(t) \right) \\ &= \delta_{ij} \delta_{kl} x_l = \delta_{ij} x_k. \end{aligned} \quad (64)$$

Thus if write \mathbf{e}^i as the i -th coordinate Euclidean canonical vector (i.e., $(\mathbf{e}^i)_j = \delta_{ij}$), then one can have

$$\begin{aligned} \left. \frac{\partial \mathbf{f}}{\partial \mathbf{W}} \right|_{(\mathbf{x}^*, \mathbf{W}^*)} : \delta \mathbf{W} &= \sum_{i,j,k} \delta_{ij} x_k^* (\mathbf{e}^i \otimes \mathbf{e}^j \otimes \mathbf{e}^k) : \sum_{l,m} \delta W_{lm} (\mathbf{e}^l \otimes \mathbf{e}^m) \\ &= \sum_{i,j,k,l,m} \delta_{ij} x_k^* \delta_{jl} \delta_{km} \delta W_{lm} \mathbf{e}^i = \sum_{i,j,k} \delta_{ij} x_k^* \delta W_{jk} \mathbf{e}^i \\ &= \sum_{i,k} \delta W_{ik} x_k^* \mathbf{e}^i = \delta \mathbf{W} \mathbf{x}^*. \end{aligned} \quad (65)$$

By similar computations, for remaining terms one can easily verify that $\left. \frac{\partial \mathbf{g}}{\partial \mathbf{x}} \right|_{(\mathbf{x}^*, \mathbf{x}_\tau^*, \mathbf{W}^*)} \cdot \delta \mathbf{x} = \rho (\delta \mathbf{x} \mathbf{x}_\tau^{*\top} - \mathbf{x}_\tau^* \delta \mathbf{x}^\top)$, $\left. \frac{\partial \mathbf{g}}{\partial \mathbf{x}_\tau} \right|_{(\mathbf{x}^*, \mathbf{x}_\tau^*, \mathbf{W}^*)} \cdot \delta \mathbf{x}_\tau = \rho (\mathbf{x}^* \delta \mathbf{x}_\tau^\top - \delta \mathbf{x}_\tau \mathbf{x}^{*\top})$, and $\left. \frac{\partial \mathbf{g}}{\partial \mathbf{W}} \right|_{(\mathbf{x}^*, \mathbf{x}_\tau^*, \mathbf{W}^*)} : \delta \mathbf{W} = -\gamma \delta \mathbf{W}$. Therefore summing up the results, we finally get

$$\boxed{\begin{cases} \dot{\delta \mathbf{x}} = (-\mathbf{I} + \mathbf{W}^*) \delta \mathbf{x} + \delta \mathbf{W} \mathbf{x}^* \\ \dot{\delta \mathbf{W}} = -\gamma \delta \mathbf{W} + \rho (\delta \mathbf{x} \mathbf{x}_\tau^{*\top} - \mathbf{x}_\tau^* \delta \mathbf{x}^\top + \mathbf{x}^* \delta \mathbf{x}_\tau^\top - \delta \mathbf{x}_\tau \mathbf{x}^{*\top}), \end{cases}} \quad (66)$$

and this is the variational equation, Eq. (10). ■

C2: Computational Method for Estimating Maximal Lyapunov Exponent

The method of computation directly follows [26]. First, the DDE (10), say, $\dot{\mathbf{U}} = \mathbf{F}(\mathbf{U}, \mathbf{U}_\tau)$, where $\mathbf{U} \in \mathbb{R}^{N+N^2}$ represents the collection of all components of $\delta \mathbf{x}$ and $\delta \mathbf{W}$, can be approximated with some conjugate discrete finite dimensional map

$$\bar{\mathbf{F}} : \underbrace{\mathbb{R}^{N+N^2} \times \dots \times \mathbb{R}^{N+N^2}}_d \rightarrow \underbrace{\mathbb{R}^{N+N^2} \times \dots \times \mathbb{R}^{N+N^2}}_d, \quad (67)$$

having variables $\bar{\mathbf{U}}^n \in \mathbb{R}^{N+N^2}$, $n = 1, \dots, d$, which

$$(\bar{\mathbf{U}}^1, \dots, \bar{\mathbf{U}}^{d-1}, \bar{\mathbf{U}}^d) = (\mathbf{U}(t - (d-1)\Delta t), \dots, \mathbf{U}(t - \Delta t), \mathbf{U}(t)), \quad \left(\Delta t = \frac{\tau}{d-1} \right), \quad (68)$$

so that the each iteration $\bar{\mathbf{U}}(k+1) = \bar{\mathbf{F}}(\bar{\mathbf{U}}(k))$ for $\bar{\mathbf{U}}$ represents the mapping of $\bar{\mathbf{U}} = (\bar{\mathbf{U}}^1, \dots, \bar{\mathbf{U}}^d)$ on time t to $t + \tau + \Delta t$. As the initial choice of $\bar{\mathbf{U}}$ is given by sampled discrete points on $t \in [-\tau, 0]$, this map starts to generate the approximated solution on interval $[\Delta t, \tau + \Delta t]$, $[\tau + 2\Delta t, 2\tau + 2\Delta t]$ and so on.

The discrete map $\bar{\mathbf{F}}$ conjugate to \mathbf{F} can be found by any convenient integration techniques. Simply, for example, Euler-method integration takes

$$\begin{aligned} \bar{\mathbf{U}}^1(k+1) &= \bar{\mathbf{U}}^d(k) + \mathbf{F}(\bar{\mathbf{U}}^d(k), \bar{\mathbf{U}}^1(k)) \Delta t, \\ \text{and for } 1 < i \leq d; \quad \bar{\mathbf{U}}^i(k+1) &= \bar{\mathbf{U}}^{i-1}(k+1) + \mathbf{F}(\bar{\mathbf{U}}^{i-1}(k+1), \bar{\mathbf{U}}^i(k)) \Delta t. \end{aligned} \quad (69)$$

Now, setting $\bar{\mathbf{U}}(0)$ containing all of the discrete-sampled initial data of each $\delta \bar{\mathbf{x}}_i$, $\delta \bar{\mathbf{W}}_{ij} \in \mathbb{R}^d$ and obtaining the evolution of $\bar{\mathbf{U}}$ for each step, then the rate of exponential growth of universal deviation (the collection of every deviations)

$$[\bar{\mathbf{U}}](k) = [\delta \bar{\mathbf{x}}_1(k); \dots; \delta \bar{\mathbf{x}}_N(k); \delta \bar{\mathbf{W}}_{11}(k); \dots; \delta \bar{\mathbf{W}}_{NN}(k)] \in \mathbb{R}^{d(N+N^2)} \quad (70)$$

where ‘;’ denotes the vertical concatenation, is estimated by directly computing the value

$$\lambda_{\max} = \lim_{K \rightarrow \infty} \frac{1}{K(\tau + \Delta t)} \sum_{k=1}^K \ln \left(\frac{\|[\bar{\mathbf{U}}](k)\|}{\|[\bar{\mathbf{U}}](k-1)\|} \right). \quad (71)$$

This value λ_{\max} , turns out to be the maximal rate of exponential evolution of the universal deviation and in fact is the MLE, and its convergence as $K \rightarrow \infty$ is well known [26].

References

- [1] K. I. Blum and L. F. Abbott, “A model of spatial map formation in the hippocampus of the rat,” *Neural computation*, vol. 8, no. 1, pp. 85–93, 1996.
- [2] R. P. Rao and T. J. Sejnowski, “Spike-timing-dependent hebbian plasticity as temporal difference learning,” *Neural computation*, vol. 13, no. 10, pp. 2221–2237, 2001.
- [3] M. Tsodyks, “Spike-timing-dependent synaptic plasticity—the long road towards understanding neuronal mechanisms of learning and memory,” *Trends in neurosciences*, vol. 25, no. 12, pp. 599–600, 2002.
- [4] B. Szatmáry and E. M. Izhikevich, “Spike-timing theory of working memory,” *PLoS Comput Biol*, vol. 6, no. 8, p. e1000879, 2010.
- [5] J.-H. Han, S. A. Kushner, A. P. Yiu, H.-L. L. Hsiang, T. Buch, A. Waisman, B. Bontempì, R. L. Neve, P. W. Frankland, and S. A. Josselyn, “Selective erasure of a fear memory,” *Science*, vol. 323, no. 5920, pp. 1492–1496, 2009.
- [6] S. Ramirez, X. Liu, P.-A. Lin, J. Suh, M. Pignatelli, R. L. Redondo, T. J. Ryan, and S. Tonegawa, “Creating a false memory in the hippocampus,” *Science*, vol. 341, no. 6144, pp. 387–391, 2013.
- [7] R. L. Redondo, J. Kim, A. L. Arons, S. Ramirez, X. Liu, and S. Tonegawa, “Bidirectional switch of the valence associated with a hippocampal contextual memory engram,” *Nature*, vol. 513, no. 7518, pp. 426–430, 2014.
- [8] J. S. Kelso, *Dynamic patterns: The self-organization of brain and behavior*. MIT press, 1995.
- [9] G. G. Globus, *The postmodern brain*. J. Benjamins Publishing Company, 1995.
- [10] M. Breakspear, “Dynamic models of large-scale brain activity,” *Nature neuroscience*, vol. 20, no. 3, pp. 340–352, 2017.
- [11] T. J. Wills, C. Lever, F. Cacucci, N. Burgess, and J. O’Keefe, “Attractor dynamics in the hippocampal representation of the local environment,” *Science*, vol. 308, no. 5723, pp. 873–876, 2005.
- [12] E. T. Rolls, “An attractor network in the hippocampus: theory and neurophysiology,” *Learning & memory*, vol. 14, no. 11, pp. 714–731, 2007.
- [13] M. Tsodyks, “Attractor neural network models of spatial maps in hippocampus,” *Hippocampus*, vol. 9, no. 4, pp. 481–489, 1999.

- [14] S. Stringer, E. Rolls, and T. Trappenberg, “Self-organizing continuous attractor network models of hippocampal spatial view cells,” *Neurobiology of learning and memory*, vol. 83, no. 1, pp. 79–92, 2005.
- [15] C. Rennó-Costa, J. E. Lisman, and P. F. Verschure, “A signature of attractor dynamics in the ca3 region of the hippocampus,” *PLoS Comput Biol*, vol. 10, no. 5, p. e1003641, 2014.
- [16] E. T. Rolls, “Attractor networks,” *Wiley Interdisciplinary Reviews: Cognitive Science*, vol. 1, no. 1, pp. 119–134, 2010.
- [17] L. Susman, N. Brenner, and O. Barak, “Stable memory with unstable synapses,” *Nature communications*, vol. 10, no. 1, pp. 1–9, 2019.
- [18] H.-G. Yoon and P. Kim, “A stdp-based encoding/decoding algorithm for associative and composite data,” *arXiv preprint arXiv:2104.12249*, 2021.
- [19] P. Dayan, L. F. Abbott, *et al.*, “Theoretical neuroscience: computational and mathematical modeling of neural systems,” *Journal of Cognitive Neuroscience*, vol. 15, no. 1, pp. 154–155, 2003.
- [20] R. Kempter, W. Gerstner, and J. L. Van Hemmen, “Hebbian learning and spiking neurons,” *Physical Review E*, vol. 59, no. 4, p. 4498, 1999.
- [21] J. C. Sprott and J. C. Sprott, *Chaos and time-series analysis*, vol. 69. Citeseer, 2003.
- [22] M. Sandri, “Numerical calculation of lyapunov exponents,” *Mathematica Journal*, vol. 6, no. 3, pp. 78–84, 1996.
- [23] W. Singer and C. M. Gray, “Visual feature integration and the temporal correlation hypothesis,” *Annual review of neuroscience*, vol. 18, no. 1, pp. 555–586, 1995.
- [24] N. Gupta, S. S. Singh, and M. Stopfer, “Oscillatory integration windows in neurons,” *Nature communications*, vol. 7, no. 1, pp. 1–10, 2016.
- [25] U. Rutishauser, I. B. Ross, A. N. Mamelak, and E. M. Schuman, “Human memory strength is predicted by theta-frequency phase-locking of single neurons,” *Nature*, vol. 464, no. 7290, pp. 903–907, 2010.
- [26] J. D. Farmer, “Chaotic attractors of an infinite-dimensional dynamical system,” *Physica D: Nonlinear Phenomena*, vol. 4, no. 3, pp. 366–393, 1982.